Lifetime Measurement in Excited and Yrast Superdeformed Bands in ^{194}Hg

J. R. Hughes,[1] I. Ahmad,[2] J. A. Becker,[1] M. J. Brinkman,[1] M. P. Carpenter,[2] B. Cederwall,[3] M. A. Deleplanque,[3] R. M. Diamond,[3] J. E. Draper,[4] C. Duyar,[4] P. Fallon,[3] S. Harfenist,[2] E. A. Henry,[1] R. G. Henry,[2] R. W. Hoff,[1] R. V. F. Janssens,[2] T. L. Khoo,[2] T. Lauritsen,[2] I. Y. Lee,[3] E. Rubel,[4] F. S. Stephens,[3] and M. A. Stoyer[1]

[1]*Lawrence Livermore National Laboratory, Livermore, California 94550*

[2]*Argonne National Laboratory, Argonne, Illinois 60439*

[3]*Lawrence Berkeley Laboratory, Berkeley, California 94720*

[4]*Physics Department, University of California, Davis, California 95616*

(Received 4 October 1993)

Nuclear level lifetimes have been measured in two superdeformed bands in ^{194}Hg using the Doppler-shift attenuation method. Average transition quadrupole moments derived from the lifetimes of an excited and yrast superdeformed bands are $Q_t = 17.6(30)$ and $17.2(20)$ eb, respectively. The Doppler shifts of the excited band relative to the yrast band indicate a slight difference in quadrupole moments [+4(5)%], assuming similar side feeding. *These results imply that the second well is stable and rigid with respect to the particle excitation responsible for this excited band.*

PACS numbers: 21.10.Re, 21.10.Tg, 27.80.+w

Superdeformed (SD) rotational structures in nuclei have been the subject of intense interest since the discovery of a discrete SD rotational band in ^{152}Dy [1]. A region of superdeformation has been established in the neutron deficient Hg [2] and Pb [3] nuclei around $A \sim 190$. These SD bands are associated with a second minimum in the potential energy surface at large deformation. The second minimum is stabilized by shell gaps in the single-particle spectrum at $Z = 80$ and $N = 112$, and is calculated to persist down to low angular momentum [4].

Level lifetimes have been measured in the yrast SD bands in ^{192}Hg [5] and ^{194}Pb [6]. The results confirm that these bands are associated with a large intrinsic deformation and further indicate that the nuclear shape in the second minimum is insensitive to increasing rotational frequency. Very little information exists, however, on the effects of quasiparticle excitations on the stability and deformation of the second minimum. Recent calculations using a microscopic description of the interaction, and a three dimensional cranked Hartree-Fock (CHF) method [7], have had considerable success explaining SD properties in the $A \sim 190$ region. These calculations predict that the yrast and excited SD bands in ^{194}Hg have quadrupole moments which are equal to within 1%, and show very little dependence on angular momentum [8].

The deformation and spin dependence of the second minimum can best be determined by measuring the lifetimes of individual SD states. In the present Letter, we present the lifetime results from a Doppler-shift attenuation measurement analysis for the yrast and one excited SD band in ^{194}Hg. Three SD bands have been reported in this nucleus [9,10]. We will refer to these bands using the nomenclature of Ref. [9], where bands 2 and 3 are interpreted as signature partner bands based on the excited $[624]9/2 \otimes [512]5/2$ neutron configuration. The present results represent the first time individual transition quadrupole moments have been measured in an excited SD band: previous results have only shown that fractional shifts in one ^{191}Hg excited band are of the same order as those in the yrast band [11].

Excited states in ^{194}Hg were populated with the ^{150}Nd(^{48}Ca, $4n$) reaction at a beam energy of 205 MeV (196 MeV at midtarget). The target consisted of 1.7 mg/cm^2 ^{150}Nd evaporated onto a 20 mg/cm^2 Au backing. The front face of the target was covered with 200 μg/cm^2 Au to retard target oxidation. In-beam γ rays were detected using the early implementation phase of the GAMMASPHERE array [12]. The measurements described here were performed with 25 Compton-suppressed germanium (Ge) detectors, each located 25.5 cm from the target position, and subtending ~ 58 msr. The number of Ge detectors n at each angle θ with respect to the beam direction is (5, 163°), (5, 148°), (5, 143°), (5, 32°), and (5, 17°). Approximately 4×10^8 expanded threefold events were recorded with this experimental setup.

The threefold data were subsequently double gated by pairs of fully stopped coincident clean SD transitions in each band, and sorted into spectra consisting of coincidences between events in detectors at backward angles with all other detectors, and detectors at forward angles with all other detectors. The coincidence gates used for band 1 were all combinations of those placed on the 254-, 296-, 338-, 378-, and 417-keV transitions, and for band 2 were all combinations of those on the 201-, 243-, 284-, 324-, 364-, and 403-keV transitions. From these data, the fractions of full Doppler shift $F(\tau)$ have been obtained, and line shapes of individual γ rays have been analyzed to determine the dependence of the transition quadrupole moment on rotational frequency, and to obtain information on the side-feeding lifetimes.

The $F(\tau)$ values have been obtained for almost the full range ($0 \rightarrow 100\%$) in both SD bands, as shown in Fig. 1(a). Transitions in both bands with $E_\gamma < 430$ keV

0031-9007/94/72(6)/824(4)$06.00

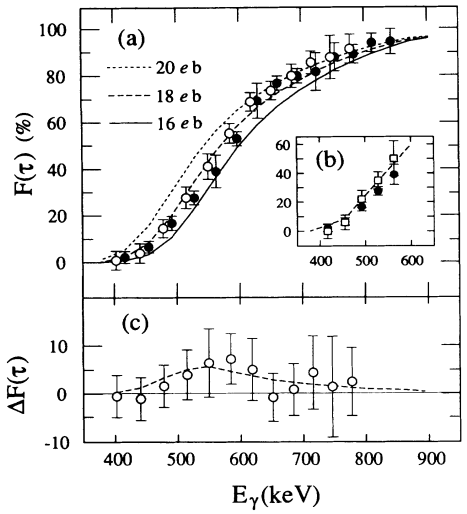

FIG. 1. (a) Measured fractional Doppler shifts for transitions in band 1 (•) and band 2 (○). The curves represent calculated values for $Q_t = 16$ (——), 18 (– – –), and 20 eb (– – – –). (b) Shifts in band 1 obtained from spectra gated by fully stopped transitions (•), and from spectra gated on high-lying moving transitions (□). (c) The difference $\Delta F(\tau)$ between bands 2 and 1, with the calculated value (– – –) appropriate for $\Delta Q_t = 0.7$ eb.

appear as sharp lines in the spectra, indicating that these decays take place after the recoiling ^{194}Hg residuals have stopped in the Au backing (in ~ 1.9 ps). For transitions with $E_\gamma > 430$ keV, however, Doppler-shifted centroids are observed, corresponding to partial in-flight decay. In band 1, the two highest measurable transitions (813 and 842 keV) show $\sim 95\%$ of the full Doppler shift expected for this reaction-target combination, with the calculated maximum recoil velocity $v/c = 2.28\%$. This indicates a total feeding time of ~ 50 fs into the top of the band. The two highest measurable transitions in band 2 (748 and 778 keV) show $\sim 90\%$ of the full Doppler shift.

The fractional shifts in band 2 are clearly very similar to those in band 1. The difference $\Delta F(\tau)$, calculated as the difference between the $F(\tau)$ in band 2 and the linearly interpolated value in band 1, is shown in Fig. 1(c). The average $\Delta F(\tau)$, 4(5)%, is independent of systematic errors and model assumptions. While this value is consistent with zero, the probability that the $F(\tau)$ in band 2 is larger than that in band 1 is $\sim 80\%$. The $\Delta F(\tau)$ is sensitive to differences in the side-feeding lifetimes and the relative Q_t in the two bands. Assuming similar side-feeding lifetimes into the two bands, the $\Delta F(\tau)$ values imply that band 2 has a slightly larger Q_t than that of band 1 [$\Delta Q_t = 0.7(9)$ e b]. The calculated $\Delta F(\tau)$ for $\Delta Q_t = 0.7$ eb is shown in Fig. 1(c). The data appear to systematically follow the $\Delta Q_t = 0.7$ eb curve, but given the errors are also consistent with $\Delta Q_t = 0$ eb.

Calculated $F(\tau)$ curves are also presented in Fig. 1(a). These curves correspond to the decay of a rotational cascade with the same dynamic moment of inertia as the two SD bands, along with a constant in-band Q_t. The side-feeding lifetimes are assumed to be the same as those in band. Calculations are presented for a number of different Q_t values. The data, however, exhibit a systematic deviation from the calculated values between the low and high recoil-energy regions for both bands. The transition is rather abrupt at $F(\tau) \sim 50\%$, corresponding to a recoil velocity $v/c \sim 1.1\%$. As a consequence, $Q_t \sim 19$ eb at high energies and $Q_t \sim 17$ eb at lower energies provide the best fit to the data for band 1. This deviation may be due to an inexact knowledge of the stopping powers, since the nuclear component to the stopping power is becoming important at $v/c \sim 1\%$.

Another possible cause for this deviation is that the side-feeding level lifetimes may be different from those of the SD levels. To investigate the effects of side feeding, spectra for band 1 were produced by gating on the top three observed transitions. These gating requirements remove the effects of side feeding into the lower levels. The statistics in these spectra are such that it was only possible to extract centroid shifts [shown in Fig. 1(b)] up to and including the 564-keV transition. The errors on these centroid shifts are large, but it appears that the 492-, 528-, and 564-keV transitions have larger centroid shifts when the effects of side feeding are removed. This indicates that the side feeding into these levels is slower than the in-band feeding. There were too few counts to apply a similar gating method in band 2. Since a similar deviation from the calculated values occurs in this band in the same spin region, however, it may be reasonable to assume that a similar effect is occurring. From a χ^2 comparison of the data to these curves, $Q_t = 17.3(20)$ eb for band 1 and $Q_t = 18.0(20)$ eb for band 2 are obtained. The effects of the systematic deviation between the data and calculated curves are not reflected in the χ^2 value, which assumes a normal distribution. The quoted errors have been corrected accordingly.

A line-shape analysis has been performed to determine individual transition quadrupole moments for the SD band members. Such an analysis is possible for the SD transitions in each band in the energy range $430 < E_\gamma < 650$ keV, where line shapes are observed; above this energy range the transitions showed no stopped component, and the analysis reduces to that of a centroid shift. Level lifetimes were extracted from these line shapes using the code DSAMFT_OR [13]. Nuclear and electronic stopping powers were calculated using the compilation of Ziegler [14]. The detailed slowing down history of ^{194}Hg recoils in the target and backing material was simulated using Monte Carlo techniques (5000 histories with a time step of 0.002 ps), and then sorted according to the detector geometry. Calculated line shapes for each in-band transition were obtained assuming both (1) a precursor cascade of rotational transitions extending to $I = 50\hbar$ feeding the top of the band, and (2) side feeding into each state modeled by a cascade of five transitions. The level lifetimes of the side-feeding cascade are parametrized by

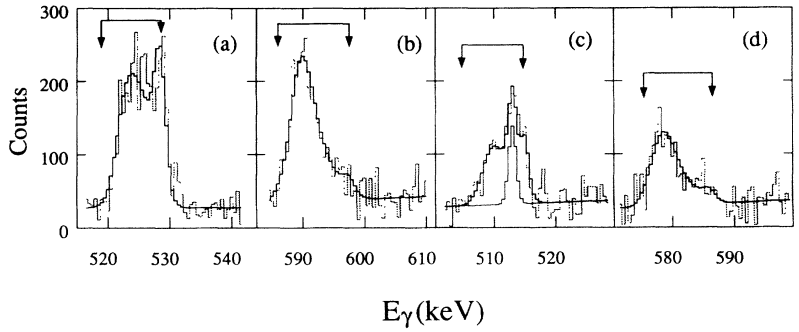

FIG. 2. Sample line-shape fits obtained at backward angles for selected transitions. The data are shown in gray, and the fits in black for the (a) 528-keV and (b) 597-keV transitions in band 1, and the (c) 515-keV and (d) 585-keV transitions in band 2. Arrows indicate the positions of stopped and fully shifted (at lower energy) components of the line shape. Note the stopped 513-keV contaminant γ-ray in the line shape of the 515-keV transition (c), which is taken into account in the fitting procedure.

$(Q_t^2/E_\gamma^5)_{\rm SF}$, where the γ-ray energies E_γ are set equal to the corresponding in-band energies. The intensity of the side feeding was constrained to the experimentally observed values. The results have been obtained from simultaneous fits to forward- and backward-angle spectra. For each transition the in-band lifetime, along with that of the side-feeding, has been determined using a χ^2 minimization technique. Examples of experimental line shapes, along with the corresponding calculated line shape, are presented in Fig 2. It is apparent that the experimental line shapes are well reproduced.

The results obtained from this analysis are summarized in Table I. For each level the deexciting transition energy, the level lifetime, and the reduced transition probability are listed. The large $B(E2)$ values confirm the collective nature of both bands, and suggest an interpretation based on the rotational model. With this assumption, the quadrupole moments can be related to the level lifetimes using $Q_t = [1.22\tau E_\gamma^5\langle IK20 \mid (I-2)K\rangle^2]^{-1/2}$, where the level lifetime (τ) is in ps, the transition energy (E_γ) is in MeV, and Q_t is in e b. The spin values (I) are those determined in Ref. [10], using the method outlined in Ref. [15], and $K = 0, 2$ [9] has been used for bands 1 and 2, respectively. The in-band and side-feeding Q_t deduced in this manner are also listed in Table I. The values obtained for $(Q_t)_{\rm SF}$ are generally smaller than the in-band Q_t in the 500 to 650 keV energy range, indicating that the side-feeding lifetimes are longer than the in-band lifetimes. A similar effect has been noted in ^{192}Hg by Moore *et al.* [5]. The $(Q_t)_{\rm SF}$ have large errors in this region since the side-feeding intensity is only (10–20)% of the in-band feeding. This is consistent, however, with the rise in $F(\tau)$ observed in the centroid-shift analysis of the spectra gated by high-spin transitions. For the higher-spin states, however, where the side-feeding intensity is comparable to the in-band feeding, $(Q_t)_{\rm SF} \approx Q_t$ gives the best fit to the data.

The individual quadrupole moments for both bands are plotted against E_γ in Fig. 3. The average in-band Q_t ob-

TABLE I. Line-shape analysis results for band 1 (upper part) and band 2 (lower part). The quoted errors contain statistical errors in the data and errors associated with the fitting procedure, but do not contain the errors inherent in the stopping powers.

E_γ (keV)	τ (ps)	Q_t (e b)	$B(E2)$ (W.u.)	$(Q_t)_{\rm SF}$ (e b)
455	0.390(92)	$17.3^{+2.5}_{-1.7}$	1570^{+490}_{-300}	d
492	0.240(32)	$18.1^{+1.3}_{-1.1}$	1730^{+270}_{-200}	d
528	0.174(36)	$17.8^{+2.2}_{-1.6}$	1670^{+440}_{-290}	13(6)
564[a]	0.164(56)	$15.6^{+3.6}_{-2.1}$	1290^{+670}_{-330}	11(6)
597	0.112(25)	$16.3^{+2.2}_{-1.6}$	1410^{+400}_{-260}	11(5)
630[b]	0.087(31)	$16.1^{+4.0}_{-2.3}$	1380^{+770}_{-360}	10(6)
662	0.060(19)	$17.2^{+3.6}_{-2.2}$	1570^{+730}_{-380}	15(5)
694	0.037(16)	$19.5^{+6.4}_{-3.2}$	2010^{+1540}_{-610}	> 18
440	0.389(132)	$19.0^{+4.3}_{-2.6}$	1860^{+950}_{-470}	d
478	0.290(70)	$17.9^{+2.6}_{-1.8}$	1660^{+530}_{-320}	d
515[c]	0.186(76)	$18.5^{+5.5}_{-2.9}$	1780^{+1230}_{-520}	15(7)
550	0.145(48)	$17.7^{+3.9}_{-2.3}$	1640^{+810}_{-410}	14(7)
585	0.129(28)	$16.1^{+2.1}_{-1.5}$	1350^{+370}_{-240}	14(6)
620	0.094(41)	$16.3^{+5.4}_{-2.7}$	1390^{+1080}_{-420}	14(6)

[a]Line shape contaminated by the 565-keV transition.
[b]Line shape contaminated by the 637-keV transition.
[c]Line shape contaminated by the 513-keV transition.
[d]No side-feeding intensity observed in these levels.

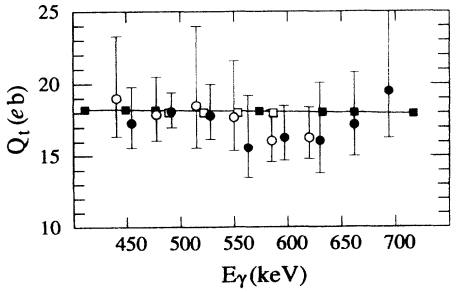

FIG. 3. Experimental transition quadrupole moment, Q_t, as a function of γ-ray energy for band 1 (•) and band 2 (○). Theoretical values calculated with the CHF method including pairing [8] for band 1 (■) and band 2 (□). A line joins the calculated values for band 1.

served for band 1 is $Q_t = 17.2(20)\ e\,\mathrm{b}$, whereas for band 2 the average is $Q_t = 17.6(30)\ e\,\mathrm{b}$. These values are consistent with those obtained from the centroid-shift analysis, and imply a quadrupole deformation $\beta_2 \sim 0.5$ using relationships given in Ref. [16]. Calculated quadrupole moments using the CHF method including pairing [8] are also shown in Fig. 3, and are essentially constant with frequency. These theoretical values reproduce the experimental values over the measured frequency range.

The calculated values predict that the quadrupole moments of the yrast and excited SD bands are the same to within 1%. This degree of sensitivity is beyond our experimental limits: from the centroid-shift data, which are subject to smaller errors than the line-shape data, we estimate that the average difference is 4(5)%. This is, perhaps, not a surprising result for the configuration containing the [624]9/2 and [512]5/2 neutron excitations. Both these orbitals are insensitive to increasing rotational frequency [9], and have only a moderate positive slope with increasing quadrupole deformation. This indicates that these orbitals each possess a small negative quadrupole moment (i.e., an oblate topology), the polarization effects of which will be small. This is certainly the case in the CHF calculations mentioned above. Nevertheless, the fact that the quadrupole moment is independent of spin and shows only a small difference with quasiparticle excitations is indicative of a stable and rigid second minimum.

A systematic picture for the yrast SD bands in Hg nuclei is now emerging; average quadrupole moments have also been reported in ^{190,191}Hg [2,11,17]. The value reported in ^{192}Hg [$Q_t = 20(2)\ e\,\mathrm{b}$] is somewhat larger than in the other isotopes [$Q_t = 17 - 18(2)\ e\,\mathrm{b}$]. A similar situation exists in the Pb nuclei where the Q_t in ^{194}Pb [6] is larger than that in ^{196}Pb [18]. As suggested in Ref. [18], a larger Q_t at $N = 112$ may be expected due to the shell gap, but with the present data, the average Q_t for these SD bands is, within errors, constant with neutron number.

In conclusion, we have measured lifetimes in the yrast and one excited SD band in ^{194}Hg. The $B(E2)$ values obtained for the excited SD band are very similar to those in the yrast band. For both bands these values are consistent with those expected for superdeformed shapes. The $F(\tau)$ values suggest there may be a slight enhancement in the Q_t of band 2, assuming similar side feeding. The results are generally consistent with CHF calculations with pairing, and indicate a rather rigid second minimum in the potential-energy surface. *This may not be the case for superdeformed bands built on other configurations. For example, it would be interesting to obtain a measure of the stability of the deformation for configurations with strongly deformation-driving orbitals.*

We would like to thank P.-H. Heenen for making available the CHF (with pairing) results prior to publication. We thank John Greene for fabricating the targets. This work was supported in part by U.S. Department of Energy, under Contract No. W-7405-ENG-48 (LLNL) and No. DE-AC03-76SF00098 (LBL), and in part by the U.S. Department of Energy, Nuclear Physics Division under Contract No. W-31-109-ENG-38 (ANL), and in part by the National Science Foundation (Davis).

[1] P.J. Twin *et al.*, Phys. Rev. Lett. **57**, 811 (1986).
[2] R.V.F. Janssens and T.L. Khoo, Annu. Rev. Nucl. Part. Sci. **41**, 321 (1991).
[3] E.A. Henry *et al.*, in *Proceedings of the International Conference on Nuclear Structure at High Angular Momentum, Ottawa, 1992* (Report No. AECL 10613, 1992), Vol. 2, p. 15.
[4] P. Bonche *et al.*, Nucl. Phys. **A500**, 308 (1989); R.R. Chasman, Phys. Lett. B **219**, 227 (1989); W. Satula *et al.*, Nucl. Phys. **A529**, 289 (1991).
[5] E.F. Moore *et al.*, Phys. Rev. Lett. **64**, 3127 (1990); I.Y. Lee *et al.*, in Ref. [3], p. 21; P. Willsau *et al.* (to be published).
[6] P. Willsau *et al.*, Z. Phys. A **344**, 351 (1993).
[7] B.-Q. Chen *et al.*, Phys. Rev. C **46**, R1582 (1992).
[8] B. Gall *et al.* (private communication).
[9] M.A. Riley *et al.*, Nucl. Phys. **A512**, 178 (1990).
[10] C.W. Beausang *et al.*, Z. Phys. A **335**, 325 (1990); E.A. Henry *et al.*, Z. Phys. A **335**, 361 (1990).
[11] M.P. Carpenter *et al.*, Phys. Lett. B **240**, 44 (1990).
[12] I.Y. Lee, Nucl. Phys. **A520**, 641c (1990).
[13] DSAMFT_OR, original code by J.C. Bacelar, modified by J. Gascon and by J.C. Wells; J.C. Wells (private communication).
[14] J.F. Ziegler, *The Stopping and Range of Ions in Matter* (Pergamon Press, New York, 1980), Vols. 3 and 5.
[15] J.A. Becker *et al.*, Phys. Rev. C **41**, R9 (1990).
[16] K.E.G. Löbner, M. Vetter, and V. Hönig, Nucl. Data Tables A **7**, 495 (1970).
[17] M.W. Drigert *et al.*, Nucl. Phys. **A530**, 452 (1991).
[18] E.F. Moore *et al.*, Phys. Rev. C **48**, 2261 (1993).